Letter

Telling different unravelings apart via nonlinear quantum-trajectory averages

Eloy Piñol,[1,*] Th. K. Mavrogordatos,[1,2,*,†] Dustin Keys,[3] Romain Veyron,[1] Piotr Sierant,[1] Miguel Angel García-March,[4] Samuele Grandi,[1] Morgan W. Mitchell,[1,5] Jan Wehr,[3] and Maciej Lewenstein[1,5,‡]

[1]*ICFO – Institut de Ciències Fotòniques, The Barcelona Institute of Science and Technology, 08860 Castelldefels (Barcelona), Spain*

[2]*Department of Physics, AlbaNova University Center, SE 106 91 Stockholm, Sweden*

[3]*Department of Mathematics, The University of Arizona Tucson, Arizona 85721-0089, USA*

[4]*Instituto Universitario de Matemática Pura y Aplicada, Universitat Politècnica de València, Camino de Vera, s/n, 46022 Valencia, Spain*

[5]*ICREA – Institució Catalana de Recerca i Estudis Avançats, 08010 Barcelona, Spain*

(Received 11 December 2023; accepted 22 August 2024; published 6 September 2024)

The Gorini-Kossakowski-Sudarshan-Lindblad master equation (ME) governs the density matrix of open quantum systems (OQSs). When an OQS is subjected to weak continuous measurement, its state evolves as a stochastic quantum trajectory, whose statistical average solves the ME. The ensemble of such trajectories is termed an unraveling of the ME. We propose a method to operationally distinguish unravelings produced by the same ME in different measurement scenarios, using nonlinear averages of observables over trajectories. We apply the method to the paradigmatic quantum nonlinear system of resonance fluorescence in a two-level atom. We compare the Poisson-type unraveling, induced by direct detection of photons scattered from the two-level emitter, and the Wiener-type unraveling, induced by phase-sensitive detection of the emitted field. We show that a quantum-trajectory-averaged variance is able to distinguish these measurement scenarios. We evaluate the performance of the method, which can be readily extended to more complex OQSs, under a range of realistic experimental conditions.

DOI: 10.1103/PhysRevResearch.6.L032057

Introduction. Quantum systems interacting with Markovian environments are ubiquitous in the physical sciences. A main tool for studying their dynamics is the deterministic Gorini-Kossakowski-Sudarshan-Lindblad (GKSL) master equation (ME) [1,2]. This specifies the time evolution of the density matrix $\rho(t)$ as the system experiences both coherent and incoherent processes, with the latter involving leakage of state information to the environment [3–6]. Despite its generality and wide use, the GKSL ME does not fully describe the quantum dynamics when the environment includes measurement devices, which convert a portion of the leaked information to usable form. The temporal evolution conditioned on the measurement record m defines a quantum trajectory, in the ideal case [7] expressed as the pure state $\rho_m(t) = |\psi_m(t)\rangle\langle\psi_m(t)|$. Averaging $\rho_m(t)$ over the measurement record solves the GKSL ME [8]. The identification of the $\rho(t)$ with the ensemble average of $\rho_m(t)$ is an example of an unraveling of the ME into a stochastic equation for the pure state $\rho_m(t)$ [9–18]. Evidently, different measurement schemes correspond to different unravelings and lead to different ensembles of quantum trajectories. Unravelings thus complement the picture drawn from their corresponding ME which speaks of an unconditional evolution.

Quantities that are linear in the density matrix $\rho(t)$, such as averages of observables, are fully determined by the GKSL ME and, therefore, are independent of the choice of the unraveling dictated by a given measurement scheme. In this Letter, we develop nonlinear measures to differentiate unravelings, thus opening a way to access the physics beyond the ME. We demonstrate that evaluating an expectation value of a physical observable for a specified quantum trajectory $\rho_m(t)$, performing a nonlinear operation on the obtained result, and averaging the result over the measurement record yields a quantity that allows for distinguishing different unravelings of the same GKSL ME. We focus on a paradigmatic open quantum system, the resonance fluorescence of a two-level atom, and consider unravelings corresponding to direct photodetection and to homodyne/heterodyne detection. We remark that while direct photodetection enjoys an obvious link with intensity correlations, measuring the spectrum of squeezing is inherently tied with homodyne detection, which provides a phase reference to a phase-dependent phenomenon [19].

The unravelings. Electron shelving [20,21] paved the way to the first observations of quantum jumps [22–24], followed by several atomic [25–27] and solid-state physics experiments [28–30]. The theoretical description of these investigations dates back to early works [31–42] that stimulated the development of quantum trajectory theory [10,43–50]. Two unravelings of the GKSL ME that play a fundamental role in

*These authors contributed equally to this work.
†Contact author: themis.mavrogordatos@fysik.su.se
‡Contact author: maciej.lewenstein@icfo.es

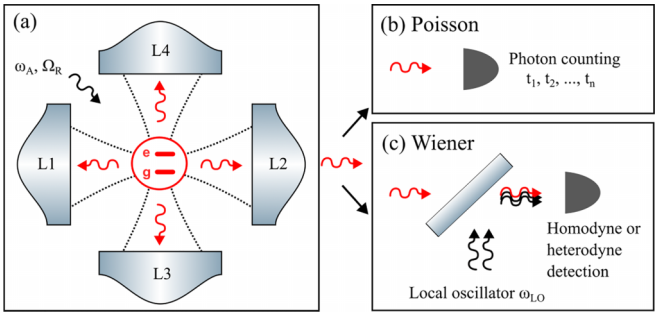

FIG. 1. *Schematic representation of the two main unraveling schemes.* In this setup, the trapped two-state atom is illuminated in a Maltese-cross arrangement [51,52] shown in (a). The output radiation escaping a particular lens is directed to either (b) a collection of avalanche photodetectors (APDs) producing a time series of "click" events (Poisson-type unraveling) or (c) a mixer with a strong local oscillator field, to substantiate either a homodyne ($\omega_{\rm LO} = \omega_A$) or a heterodyne measurement ($|\omega_{\rm LO} - \omega_A| \gg \gamma$) scheme (Wiener-type unraveling).

the understanding of the quantum trajectories are (i) Poisson unraveling, related to direct photodetection and the so called quantum Monte Carlo wave function approach [12,53–56]; and (ii) Wiener-type unraveling (the quantum state diffusion model proposed by Gisin and Percival) [57,58], relating conditional quantum dynamics to a continuous Wiener process [59]. In the context of atomic physics experiments, the distinct unravelings correspond to different photodetection schemes [5], see Fig. 1. The Poisson unraveling is relevant for the direct photodetection experiments, while the continuous Wiener process arises in homodyne and heterodyne photodection schemes [10,60].

The disparity between the experimental setups is reflected in the different nature of quantum trajectories [58]. The Wiener process yields a continuous evolution of the system state $|\psi(t)\rangle$. In contrast, the acts of direct photodetection at times $t_1 < t_2 < \ldots < t_n$ collapse the conditional wavefunction. The resulting time evolution of $|\psi(t)\rangle$ is discontinuous and the final state at $t > t_n$ depends, in general, on a particular sequence of emission times $|\psi(t)\rangle = |\psi_{t_1,\ldots,t_n}(t)\rangle$. By collecting photon counting records, the experimenter effectively determines the quantum trajectory of the atom. The entanglement between the electromagnetic field and the atom is the key ingredient that allows for the inference of the atom's state based on the photodetection events [58,61]. In particular, Nha and Carmichael demonstrated that the degree of entanglement depends on how information in the environment is read [61].

Source master equation and linear averages. Our starting point is the GKSL ME of resonance fluorescence, governing the (unconditional) dynamics of the reduced system density matrix ρ,

$$\frac{d\rho}{dt} = \mathcal{L}\rho = -i\frac{1}{2}\omega_A[\sigma_z, \rho] - i\Omega[e^{-i\omega_A t}\sigma_+ + e^{i\omega_A t}\sigma_-, \rho] + \frac{\gamma}{2}(2\sigma_-\rho\sigma_+ - \sigma_+\sigma_-\rho - \rho\sigma_+\sigma_-), \quad (1)$$

where we have neglected thermal excitation [62]. In the ME (1), $\sigma_+, \sigma_-, \sigma_z$ are the raising, lowering, and inversion operators (represented by Pauli matrices), respectively, for the two-level atom coherently driven by a resonant laser field of frequency ω_A; $\Omega_R = 2\Omega$ is the Rabi frequency at which the two-state atom periodically oscillates between its ground and excited states; and γ is the spontaneous emission rate. The solution of the corresponding optical Bloch equations yields the following expression for the average inversion when the atom is initialized in its ground state:

$$\overline{\langle\sigma_z(t)\rangle} = S_z\left[1 + Y^2 e^{-(3\gamma/4)t}\left(\cosh\delta t + \frac{(3\gamma/4)}{\delta}\sinh\delta t\right)\right], \quad (2)$$

where $Y \equiv \sqrt{2}\Omega_R/\gamma$, $\delta \equiv \frac{\gamma}{4}\sqrt{1 - 8Y^2}$, and $S_z = -1/(1 + Y^2)$ is the steady-state inversion. Hereinafter, we denote by $\langle\cdot\rangle$ the quantum mechanical average over an individual realization. For strong driving ($Y \gg 1$) the average inversion exhibits damped oscillations at Ω_R, relaxing to $0 + \mathcal{O}(\gamma^2/\Omega^2)$. Equation (2) is an example of a typical linear average computed directly from the ME, against which our nonlinear averages are to be compared. We now describe the nonlinear averages.

Nonlinear averages beyond the density-matrix formalism. The idea underlying our approach is to perform a nonlinear operation on a quantum mechanical expectation value evaluated for an individual quantum trajectory prior to averaging of the result over the ensemble of quantum trajectories denoted by $\overline{(\circ)}$. A characteristic nonlinear average of our focus is the quantity $\mathrm{Var}(\sigma_z) \equiv \overline{\langle\sigma_z(t)\rangle^2} - [\overline{\langle\sigma_z(t)\rangle}]^2$, which we hereinafter call quantum-trajectory-averaged variance (QTAV).

The results depicted in Fig. 2 substantiate the pivotal influence of the environment when collecting records of a strongly driven two-state atom and taking a sum over a collection of them. The two principal unravelings are presented in their ability to produce an ostensibly disparate $\mathrm{Var}(\sigma_z)$, while the corresponding average inversion remains unchanged. For the direct photodetection [63–65], corresponding to the Poisson-type unraveling of the ME, we obtain an exact expression for $\mathrm{Var}(\sigma_z)$ based on the waiting-time distribution [38,66]. For $\gamma t \gg 1$, the asymptotic expression for the variance, including first-order terms in γ/Ω of different frequencies, reads [62]

$$\mathrm{Var}(\sigma_z) = \frac{1}{2}\left\{1 + e^{-\gamma t/2}\cos(4\Omega t) + \frac{\gamma}{8\Omega}e^{-\gamma t/2}[4\sin(4\Omega t) - \sin(6\Omega t) - 3\sin(2\Omega t)] + \mathcal{O}(\gamma^2/\Omega^2)\right\}. \quad (3)$$

The first observation to be made from Eq. (3) is that the amplitude of the dominant term (second term in the sum) to the QTAV—revealing a frequency doubling with respect to the inversion—is independent of Ω. The variance ultimately relaxes to $1/2$, as we can see in both uppermost panels of frames (a) and (b). The asymptotic evolution to the steady state is in very good agreement with the exact Monte Carlo simulations as well as with the perturbative treatment of the Dyson-series expansion for the variance [62], and the truncated hierarchy of moments produced from the adjoint Lindbladian.

The time evolution of the QTAV is significantly altered, see the middle panels of Fig. 2, when one places a beam splitter and a local oscillator in the environment, and the fluorescent signal interferes with the latter before photodetection [Fig. 1(c)], corresponding to the heterodyne detection and exemplifying Wiener-type unraveling. The frequency doubling

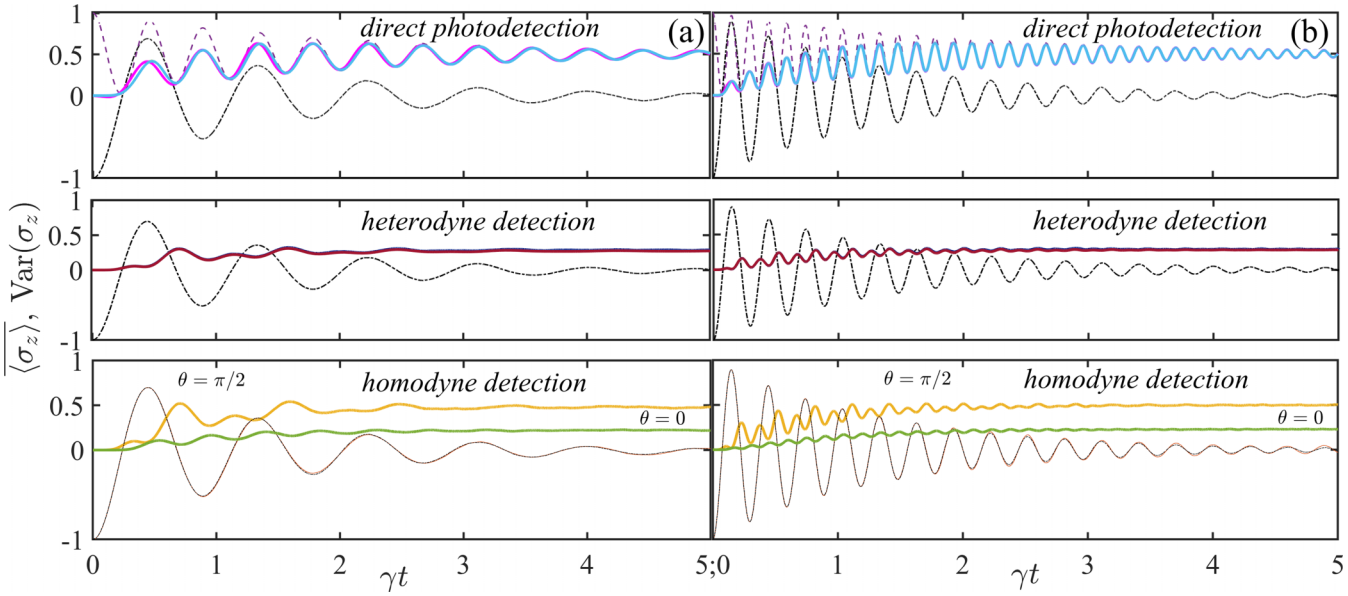

FIG. 2. *Linear vs nonlinear quantum-trajectory averages for three principal unravelings.* Monte Carlo averages over 10^4 realizations of the QTAV $\mathrm{Var}(\sigma_z)$ plotted against the dimensionless time γt for a Poisson-type unraveling (direct photodetection) and two Wiener-type unravelings (homodyne and heterodyne detection) as indicated in each panel, for (a) $Y = 10$ and (b) $Y = 30$, with the two-level atom initialized in its ground state. The oscillatory dot-dashed curves with alternating sign in all frames depict the average inversion $\overline{\langle\sigma_z(t)\rangle}$. In the uppermost panels of both frames, the pink and blue curves depict $\mathrm{Var}(\sigma_z)$ obtained from the perturbative treatment of the Dyson-series expansion to first order in γ/Ω, and the moment-based equations, respectively. The latter results are indistinguishable from the Monte Carlo simulations on the scale of the figure. The dashed curves (in purple) depict the asymptotic expression (3). For heterodyne detection, the QTAV obtained from the numerical simulations (in blue) is indistinguishable from the moment-based method results (in red). Homodyne detection is performed with the local-oscillator phase selected along the antisqueezed and squeezed quadratures of the fluorescent field, at $\theta = 0$ and $\pi/2$, respectively, corresponding to the same inversion average (brown curve overlapping with the dot dashed).

is also in evidence, although the contrast in the oscillations is visibly suppressed. The light scattered by the two-level emitter is squeezed in the field quadrature that is in phase with the mean scattered field amplitude $\propto \langle\sigma_-(t)\rangle$ [67,68]. The bottom panel in each frame shows that the QTAV responds differently to the detection of the squeezed vs the direction of the antisqueezed quadrature of the fluorescent field, i.e., along an axis perpendicular to the equator of the Bloch sphere where quantum fluctuations are redistributed among the quadratures.

Ensemble moments and adjoint Lindbladian. To provide some analytical grounding to the behavior of the QTAV, we will delineate a method akin to the optical Bloch equations extended to account for the nonlinear averages. The contributions from the Itô corrections to the ensemble moments can be found easily in the Heisenberg picture [69]. Under the Poisson unraveling for an observable A [44] (we denote $\langle A(t)\rangle$ by $\langle A\rangle_t$),

$$d\langle A\rangle_t = \langle\mathcal{L}^\dagger[A]\rangle_t dt + \left(\frac{\langle\sigma_+ A\sigma_-\rangle_{t-}}{\langle\sigma_+\sigma_-\rangle_{t-}} - \langle A\rangle_{t_-}\right) d\widetilde{N}(t), \quad (4)$$

where $\widetilde{N}$ is the compensated Poisson process, $d\widetilde{N} = dN - \gamma\langle\sigma_+\sigma_-\rangle_t dt$, with a future pointing differential of expected value zero. This means that the ensemble average, here denoted by $\mathbb{E}$ for readability, is just

$$d\mathbb{E}\langle A\rangle_t = \mathbb{E}\langle\mathcal{L}^\dagger[A]\rangle_t dt,$$

which is the Heisenberg unraveling of the ME. It is useful to consider this equation for a Hilbert-Schmidt basis X_i for the space of observables. Call the quantum expectation $x_i = \langle X_i\rangle$. Thus, each observable A has a corresponding vector a such that $\langle A\rangle = (a, x)$. If we use the basis corresponding to the three Pauli matrices and the identity, all normalized in the Hilbert-Schmidt norm, then the vector for $A = \sigma_z$ is $a = (0, 0, 0, \sqrt{2})$. Since a is just a constant vector, generally we have that $\mathbb{E}\langle A\rangle = \mathbb{E}(a, x) = (a, \mathbb{E}x)$ and the square of the quantum expectation becomes $\langle A\rangle^2 = \sum_{ij} a_i a_j x_i x_j$ so that $\mathbb{E}\langle A\rangle^2 = \sum_{ij} a_i a_j \mathbb{E}x_i x_j$, and so to see how the ensemble average of square of the quantum expectation evolves in time, it is necessary to know how $\mathbb{E}x_i x_j$ evolves. In the Poisson case, we obtain

$$\begin{aligned} d\mathbb{E}x_i x_j &= \mathbb{E}(x_i\langle\mathcal{L}^\dagger[X_j]\rangle_t dt + \langle\mathcal{L}^\dagger[X_i]\rangle_t x_j dt) \\ &\quad + \mathbb{E}\left(\frac{\langle\sigma_+ X_i\sigma_-\rangle_t}{\langle\sigma_+\sigma_-\rangle_t} - x_i\right)\left(\frac{\langle\sigma_+ X_j\sigma_-\rangle_t}{\langle\sigma_+\sigma_-\rangle_t} - x_j\right) \\ &\quad \times \langle\sigma_+\sigma_-\rangle_t dt = \mathbb{E}\Big(x_i(u^j, x) + (u^i, x)x_j \\ &\quad + \frac{1}{(l, x)}((v^i, x_i) - x_i(l, x))((v^j, x) - x_j(l, x))\Big)dt, \end{aligned}$$

using the fact that $d\widetilde{N}d\widetilde{N} = dN$ with the rate of the Poisson process being $\gamma\langle\sigma_+\sigma_-\rangle_t dt$ and in the last line using u^j as the vector corresponding to $\mathcal{L}^\dagger[X_j]$, l as $\sigma_+\sigma_-$, and v^j as $\sigma_+ X_j\sigma_-$. This is an ordinary differential equation which, however, does not close since it requires higher order moments such as $\mathbb{E}x_i x_j x_k$. Again, using the Itô product rule we can calculate the equation for the higher order moments to obtain a system of ordinary differential equations which still do not close. We

can repeat this procedure to arbitrarily high order but at some point we have to truncate. It can be shown that this truncation is linear in the moments, which allows us to solve the system using traditional methods of solving linear systems of ODEs. The Wiener case [44,57,70,71] can be similarly approximately solved by using the Heisenberg equation [69]

$$d\langle A\rangle_t = \langle \mathcal{L}^\dagger[A]\rangle_t dt + \left(\sqrt{\gamma}\langle A(\sigma_- - \langle\sigma_-\rangle_t)\rangle \frac{dW(t)}{\sqrt{2}} + \text{H.c.}\right),$$

where W is a complex Wiener process. Solutions to these kind of truncated systems of equations for the two principal unravelings are depicted in Fig. 2, in very good agreement with the Dyson-expansion method and Monte Carlo averages.

Direct photodetection revisited and compromised. Having laid out an operational approach to distinguish the different unravelings, let us return to direct photodetection and discuss the most commonly encountered limitations in an actual experiment, where the density matrix cannot be unraveled into a pure-state ensemble, in which we would have a conditional wavefunction obeying a Schrödinger equation with a non-Hermitian Hamiltonian. This happens for a limited detector efficiency $\eta < 1$ and/or a surrounding bath with appreciable thermal excitation $\overline{n}$ [62].

Figure 3 testifies to the rapid degradation of $\mathrm{Var}(\sigma_z)$ as we move away from a pure-state description of the conditional dynamics. The QTAV responds to quantum jumps taking place in the course of individual realizations. This is evident from Fig. 3(b) where $\mathrm{Var}(\sigma_z)$ remains zero until a spontaneous-emission event occurs in a pair of realizations. For an imperfect detector or for a thermally excited bath, the regression of fluctuations following a jump is damped. The decay concerns the coherent part of the evolution between spontaneous emissions, at a rate much faster than γ, for typical experimental parameters where $\eta \ll 1$. The inset of Fig. 3(a) shows how sample trajectories spiral toward the center of the Bloch sphere, while individual jumps reset the evolution to the south pole.

Since the intensity correlation of the scattered light reflects a nonexclusive probability of photocounting coincidences, the limited detector efficiency can be counterbalanced by increasing the number of photon "clicks" N in the course of a long experimental run. Indeed, for the setup pictured in Fig. 1(a), we have concluded that the signal-to-noise ratio for $g^{(2)}(\gamma\tau \gg 1)$ in a window about one inverse of the coherence time scales with $\sqrt{N}$ [62]. This allows the determination of $\mathrm{Var}(\sigma_z)$ from single realizations as low as 10^{-3}, which is the order of magnitude Monte Carlo simulations indicate for $\eta \lesssim 0.05$. This order of magnitude can be increased using high numerical aperture collection systems [51,72] and efficient single-photon detectors [73].

Conclusions and outlook. In summary, we have expanded upon the fundamental concept of the variance in quantum mechanics going beyond the conventional density-matrix formulation. The different environments devised to collect the output of an open quantum system show up in a markedly different response of a quantity where nonlinear operations are performed to individual realizations prior to averaging over their ensemble. This is in contrast to linear observable averages where the complementary measurement strategies all

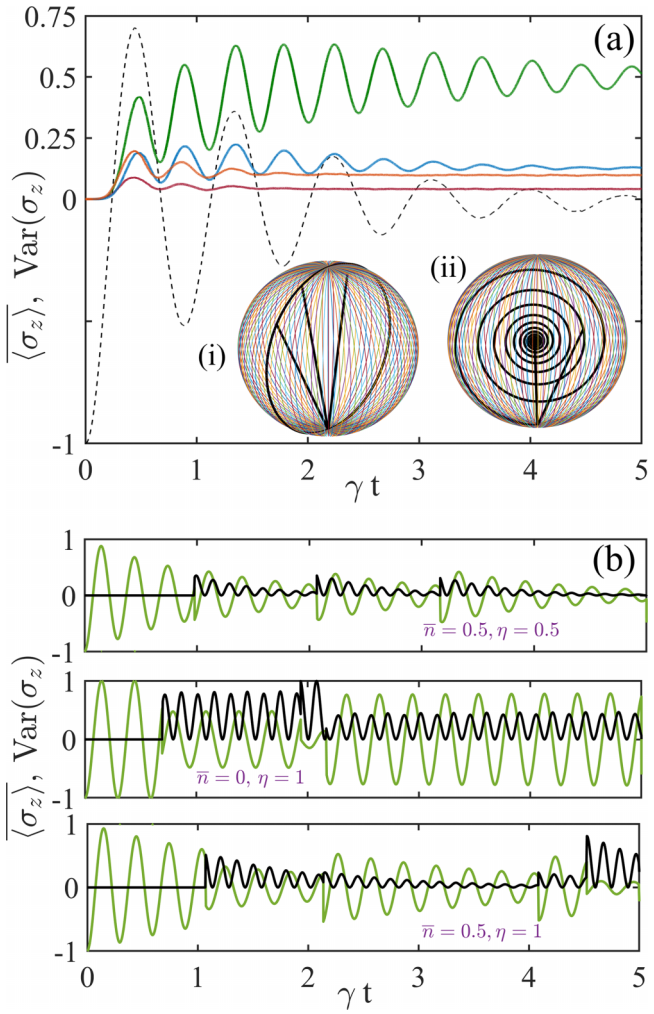

FIG. 3. *Experimental limitations and decay of "conditional" coherence.* (a) Monte Carlo average over 10^4 realizations of the QTAV $\mathrm{Var}(\sigma_z)$ obtained with $Y = 10$, plotted against the dimensionless time γt for the ideal case $\overline{n} = 0, \eta = 1$ (in green), $\overline{n} = 0, \eta = 0.5$ (in blue), $\overline{n} = 1, \eta = 1$ (in orange), and $\overline{n} = 1, \eta = 0.5$ (in red). The dashed curve depicts $\overline{\langle\sigma_z(t)\rangle}$ in the ideal case. The inset shows two sample trajectories in the Bloch sphere obtained with $Y = 30$ and for $\overline{n} = 0, \eta = 1$ (i) and $\overline{n} = 1, \eta = 0.8$ (ii). (b) Monte Carlo average over two realizations for the atomic inversion, $\overline{\langle\sigma_z(t)\rangle}$ (in green) and $\mathrm{Var}(\sigma_z)$ (in black) for the values of $\overline{n}$, η indicated in each textbox.

abide by the predictions of the GKSL equation, and multitime correlations—such as the intensity correlation function—are obtained via the quantum regression formula. Following our strategy, we need to set the initial point for two copies of the system (here a ground-state reset for direct photodetection) and then postselect the trajectories in such a way that the photocounting record is the same with satisfactory accuracy. *Ergo*, one gains, in principle, the ability to characterize the experiment's power to collapse the wavefunction and add information to the memory carried by a state conditioned on all events that have taken place along a single trajectory. This ability allows for an experimentally oriented test of the objective quantum state assumption via an EPR steering inequality; direct photodetection has been argued to be "more quantum" than its Wiener-type counterparts [74–76]. While we have

focused on two primary unravelings, the possibilities are in fact endless as different output channels open up. For example, Barchielli and Gregoratti have used a measurement-based feedback protocol to assess the non-Markovian evolution of a coherently driven and continuously monitored two-level atom. The included delay has experimental consequences, modifying the Mandel Q parameter alongside the spectrum of the emitted light [77]. In general, non-Markov open systems cannot be given a trajectory interpretation built around measured outputs, as measuring non-Markov environments interferes with the reduced system dynamics. One subclass of trivially non-Markov open systems has been recently approached using trajectories [78]. Finally, our conclusions are reflected by recent investigations of quantum many-body systems studied in the context of quantum computing and quantum simulation [79–81]. Quantum trajectories arising due to multiple measurements of the system's state, when analyzed by relevant (nonlinear) statistical measures such as entanglement entropy, exhibit phase transitions [82–89] that are not evident in the average state [90–93] unless specifically tuned feedback mechanisms are employed [94–101].

Acknowledgments. We gratefully acknowledge funding from ERC AdG NOQIA; MCIN/AEI (PGC2018-0910.13039/501100011033, CEX2019-000910-S/10.13039/501100011033, Plan National FIDEUA PID2019-106901GB-I00, Plan National STAMEENA PID2022-139099NB-I00 project funded by MCIN/AEI/10.13039/501100011033, and by the European Union NextGenerationEU/PRTR" (PRTR-C17.I1), FPI); QUANTERA MAQS PCI2019-111828-2); QUANTERA DYNAMITE PCI2022-132919 (QuantERA II Programme cofunded by European Union's Horizon 2020 program under Grant Agreement No. 101017733), Ministry of Economic Affairs and Digital Transformation of the Spanish Government through the QUANTUM ENIA project call - Quantum Spain project, and by the European Union through the Recovery, Transformation, and Resilience Plan – NextGenerationEU within the framework of the Digital Spain 2026 Agenda; Fundació Cellex; Fundació Mir-Puig; Generalitat de Catalunya (European Social Fund FEDER and CERCA program, AGAUR Grant No. 2021 SGR 01452, QuantumCAT/U16-011424, cofunded by ERDF Operational Program of Catalonia 2014-2020); Barcelona Supercomputing Center MareNostrum (FI-2023-1-0013); EU Quantum Flagship (PASQuanS2.1, 101113690); EU Horizon 2020 FET-OPEN OPTOlogic (Grant No 899794); EU Horizon Europe Program (Grant Agreement No. 101080086—NeQST), ICFO Internal QuantumGaudi project; European Union's Horizon 2020 program under the Marie Sklodowska-Curie Grant Agreement No. 847648; La Caixa Junior Leaders fellowships, La Caixa' Foundation (ID 100010434): CF/BQ/PR23/11980043; European Commission project QUANTIFY (Grant Agreement No. 101135931); Spanish Ministry of Science MCIN: project SAPONARIA (PID2021-123813NB-I00) and "Severo Ochoa" Center of Excellence CEX2019-000910-S; and Departament de Recerca i Universitats de la Generalitat de Catalunya Grant No. 2021 SGR 01453. Views and opinions expressed are, however, those of the author(s) only and do not necessarily reflect those of the European Union, European Commission, European Climate, Infrastructure and Environment Executive Agency (CINEA), or any other granting authority. Neither the European Union nor any granting authority can be held responsible for them. M.A.G.M. acknowledges funding from QuantERA II Cofund 2021 PCI2022-133004, Projects of MCIN with funding from European Union NextGenerationEU (PRTR-C17.I1) and by Generalitat Valenciana, with Ref. 20220883 (PerovsQuTe) and COMCUANTICA/007 (QuanTwin), and Red Tematica RED2022-134391-T. J.W. was partially supported by NSF Grant DMS 1911358 and by the Simons Foundation Fellowship 823539.

[1] V. Gorini, A. Kossakowski, and E. C. G. Sudarshan, Completely positive dynamical semigroups of *N*-level systems, J. Math. Phys. **17**, 821 (1976).

[2] G. Lindblad, On the generators of quantum dynamical semigroups, Commun. Math. Phys. **48**, 119 (1976).

[3] H.-P. Breuer and F. Petruccione, Stochastic unraveling of relativistic quantum measurements, in *Open Systems and Measurement in Relativistic Quantum Theory*, edited by H.-P. Breuer and F. Petruccione (Springer, Berlin, Heidelberg, 1999), pp. 81–116.

[4] S. Haroche and J.-M. Raimond, *Exploring the Quantum: Atoms, Cavities, and Photons* (Oxford University Press, Oxford, 2006).

[5] H. P. Breuer and F. Petruccione, *The Theory of Open Quantum Systems* (Oxford university press, Oxford, 2002).

[6] *Open Quantum Systems II – The Markovian Approach*, edited by S. Attal, A. Joye, and C.-A. Pillet, Lecture Notes in Mathematics Vol. 1881 (Springer, Berlin, Heidelberg, 2006).

[7] The unraveling into pure states can be performed whenever the continuous evolution in the GKSL ME is governed by a commutator with a non-Hermitian Hamiltonian, and the initial state is pure. The resulting nonlinear Schroedinger equation governing the evolution of normalized states in quantum-trajectory theory is a straightforward consequence of conditioning and is not considered to arise from any previously unknown inherent stochasticity [19].

[8] L. Accardi, I. Volovich, and Y. G. Lu, *Quantum Theory and Its Stochastic Limit* (Springer, Berlin, Heidelberg, 2013).

[9] N. Bohr, H. A. Kramers, and J. C. Slater, LXXVI. The quantum theory of radiation, The London, Edinburgh, and Dublin Philosophical Magazine and Journal of Science **47**, 785 (1924).

[10] H. Carmichael, *An Open Systems Approach to Quantum Optics* (Springer, Berlin, Germany, 1993).

[11] C. W. Gardiner, A. S. Parkins, and P. Zoller, Wave-function quantum stochastic differential equations and quantum-jump simulation methods, Phys. Rev. A **46**, 4363 (1992).

[12] J. Dalibard, Y. Castin, and K. Mølmer, Wave-function approach to dissipative processes in quantum optics, Phys. Rev. Lett. **68**, 580 (1992).

[13] R. Omnès, *The Interpretation of Quantum Mechanics* (Princeton University Press, Princeton, New Jersey, 1994).

[14] Ph. Blanchard and A. Jadczyk, Event-enhanced quantum theory and piecewise deterministic dynamics, Annalen der Physik **507**, 583 (1995).

[15] A. N. Korotkov, Continuous quantum measurement of a double dot, Phys. Rev. B **60**, 5737 (1999).

[16] M. B. Plenio and P. L. Knight, The quantum-jump approach to dissipative dynamics in quantum optics, Rev. Mod. Phys. **70**, 101 (1998).

[17] G. C. Hegerfeldt and D. G. Sondermann, Conditional Hamiltonian and reset operator in the quantum jump approach, Quantum Semiclass. Opt. **8**, 121 (1996).

[18] A. J. Daley, Quantum trajectories and open many-body quantum systems, Adv. Phys. **63**, 77 (2014).

[19] H. Carmichael, *Statistical Methods in Quantum Optics 2* (Springer, Berlin, Germany, 2008), Chap. 9, 17.

[20] D. Wineland and H. Dehmelt, Proposed 1014 delta upsilon less than upsilon laser fluorescence spectroscopy on t1+ mono-ion oscillator iii, Bull. Am. Phys. Soc. **20**, 637 (1975).

[21] H. Dehmelt, Coherent spectroscopy on a single atomic system at rest in free space II, J. Phys. Colloques **42**, C8-299 (1981).

[22] W. Nagourney, J. Sandberg, and H. Dehmelt, Shelved optical electron amplifier: Observation of quantum jumps, Phys. Rev. Lett. **56**, 2797 (1986).

[23] Th. Sauter, W. Neuhauser, R. Blatt, and P. E. Toschek, Observation of quantum jumps, Phys. Rev. Lett. **57**, 1696 (1986).

[24] J. C. Bergquist, R. G. Hulet, W. M. Itano, and D. J. Wineland, Observation of quantum jumps in a single atom, Phys. Rev. Lett. **57**, 1699 (1986).

[25] Th. Basché, S. Kummer, and C. Bräuchle, Direct spectroscopic observation of quantum jumps of a single molecule, Nature (London) **373**, 132 (1995).

[26] S. Peil and G. Gabrielse, Observing the quantum limit of an electron cyclotron: QND measurements of quantum jumps between fock states, Phys. Rev. Lett. **83**, 1287 (1999).

[27] S. Gleyzes, S. Kuhr, C. Guerlin, J. Bernu, S. Deléglise, U. Busk Hoff, M. Brune, J.-M. Raimond, and S. Haroche, Quantum jumps of light recording the birth and death of a photon in a cavity, Nature (London) **446**, 297 (2007).

[28] P. Neumann, J. Beck, M. Steiner, F. Rempp, H. Fedder, P. R. Hemmer, J. Wrachtrup, and F. Jelezko, Single-shot readout of a single nuclear spin, Science **329**, 542 (2010).

[29] R. Vijay, D. H. Slichter, and I. Siddiqi, Observation of quantum jumps in a superconducting artificial atom, Phys. Rev. Lett. **106**, 110502 (2011).

[30] Z. K. Minev, S. O. Mundhada, S. Shankar, P. Reinhold, R. Gutiérrez-Jáuregui, R. J. Schoelkopf, M. Mirrahimi, H. J. Carmichael, and M. H. Devoret, To catch and reverse a quantum jump mid-flight, Nature (London) **570**, 200 (2019).

[31] R. J. Cook and H. J. Kimble, Possibility of direct observation of quantum jumps, Phys. Rev. Lett. **54**, 1023 (1985).

[32] H. J. Kimble, R. J. Cook, and A. L. Wells, Intermittent atomic fluorescence, Phys. Rev. A **34**, 3190 (1986).

[33] T. Erber and S. Putterman, Randomness in quantum mechanics—nature's ultimate cryptogram? Nature (London) **318**, 41 (1985).

[34] J. Javanainen, Possibility of quantum jumps in a three-level system, Phys. Rev. A **33**, 2121 (1986).

[35] A. Schenzle, R. G. DeVoe, and R. G. Brewer, Phase-modulation laser spectroscopy, Phys. Rev. A **25**, 2606 (1982).

[36] C. Cohen-Tannoudji and J. Dalibard, Single-atom laser spectroscopy. Looking for dark periods in fluorescence light, Europhys. Lett. **1**, 441 (1986).

[37] R. J. Cook, What are quantum jumps? Phys. Scr. **T21**, 49 (1988).

[38] J. Grochmalicki and M. Lewenstein, Detection of decay processes by means of quantum-jump statistics, Phys. Rev. A **40**, 2517 (1989).

[39] J. Grochmalicki and M. Lewenstein, Detection of cavity fields by means of quantum-jump statistics, Phys. Rev. A **40**, 2529 (1989).

[40] G. C. Hegerfeldt and M. B. Plenio, Macroscopic dark periods without a metastable state, Phys. Rev. A **46**, 373 (1992).

[41] G. C. Hegerfeldt and M. B. Plenio, Coherence with incoherent light: A new type of quantum beat for a single atom, Phys. Rev. A **47**, 2186 (1993).

[42] G. C. Hegerfeldt, The quantum jump approach and some of its applications, in *Time in Quantum Mechanics*, edited by G. Muga, A. Ruschhaupt, and A. del Campo (Springer Berlin Heidelberg, Berlin, Heidelberg, 2009), Vol. 2, pp. 127.

[43] D. Keys and J. Wehr, Poisson stochastic master equation unravelings and the measurement problem: A quantum stochastic calculus perspective, J. Math. Phys. **61**, 032101 (2020).

[44] A. Barchielli and V. P. Belavkin, Measurements continuous in time and a posteriori states in quantum mechanics, J. Phys. A: Math. Gen. **24**, 1495 (1991).

[45] T. A. Brun, A simple model of quantum trajectories, Am. J. Phys. **70**, 719 (2002).

[46] A. Barchielli, Continual measurements in quantum mechanics and quantum stochastic calculus, in *Open Quantum Systems III: Recent Developments*, edited by S. Attal, A. Joye, and C.-A. Pillet (Springer, Berlin, Heidelberg, 2006), pp. 207.

[47] V. P. Belavkin, A stochastic posterior Schrödinger equation for counting nondemolition measurement, Lett. Math. Phys. **20**, 85 (1990).

[48] V.P. Belavkin and P. Staszewski, A continuous observation of photon emission, Rep. Math. Phys. **29**, 213 (1991).

[49] G. C. Ghirardi, P. Pearle, and A. Rimini, Markov processes in Hilbert space and continuous spontaneous localization of systems of identical particles, Phys. Rev. A **42**, 78 (1990).

[50] G. C. Ghirardi, A. Rimini, and T. Weber, Unified dynamics for microscopic and macroscopic systems, Phys. Rev. D **34**, 470 (1986).

[51] N. Bruno, L. C. Bianchet, V. Prakash, N. Li, N. Alves, and M. W. Mitchell, Maltese cross coupling to individual cold atoms in free space, Opt. Express **27**, 31042 (2019).

[52] M. Weber, J. Volz, K. Saucke, C. Kurtsiefer, and H. Weinfurter, Analysis of a single-atom dipole trap, Phys. Rev. A **73**, 043406 (2006).

[53] E. B. Davies, *Quantum Theory of Open Systems* (Academic Press, New York, 1976).

[54] M. D. Srinivas and E. B. Davies, Photon counting probabilities in quantum optics, Int. J. Opt. **28**, 981 (1981).

[55] P. Zoller, M. Marte, and D. F. Walls, Quantum jumps in atomic systems, Phys. Rev. A **35**, 198 (1987).

[56] R. Dum, P. Zoller, and H. Ritsch, Monte Carlo simulation of the atomic master equation for spontaneous emission, Phys. Rev. A **45**, 4879 (1992).

[57] N. Gisin and I. C. Percival, The quantum-state diffusion model applied to open systems, J. Phys. A: Math. Gen. **25**, 5677 (1992).

[58] H. J. Carmichael, Quantum jumps revisited: An overview of quantum trajectory theory, in *Quantum Future From Volta and Como to the Present and Beyond*, edited by P. Blanchard and A. Jadczyk (Springer, Berlin, Heidelberg, 1999), p. 15.

[59] R. Durrett, *Probability: Theory and Examples*, 5th ed., Cambridge Series in Statistical and Probabilistic Mathematics (Cambridge University Press, Cambridge, 2019).

[60] H. M. Wiseman and G. J. Milburn, Quantum theory of field-quadrature measurements, Phys. Rev. A **47**, 642 (1993).

[61] H. Nha and H. J. Carmichael, Entanglement within the quantum trajectory description of open quantum systems, Phys. Rev. Lett. **93**, 120408 (2004).

[62] See Supplemental Material at http://link.aps.org/supplemental/10.1103/PhysRevResearch.6.L032057 for a detailed calculation of the QTAV in the Poisson-type unraveling, via the Dyson-series expansion of the conditional reduced system density operator. We derive exact and approximate results, the latter in the limits of strong and weak driving where asymptotic expressions can be obtained. Secondly, we expand on the generality of the moment-based method applicable to the two principal types of unraveling (Poisson and Wiener). We also connect the quadrature amplitude squeezing encountered in resonance fluorescence to $\mathrm{Var}(\sigma_z)$. Finally, we take into account experimental imperfections and discuss a strategy to determine nonlinear averages in an exemplary and pioneering system of a single trapped fluorescing ^{87}Rb atom whose output radiation is collected by four high-numerical aperture lenses in a Maltese-cross arrangement.

[63] B. R. Mollow, Pure-state analysis of resonant light scattering: Radiative damping, saturation, and multiphoton effects, Phys. Rev. A **12**, 1919 (1975).

[64] R. J. Cook, Photon statistics in resonance fluorescence from laser deflection of an atomic beam, Opt. Commun. **35**, 347 (1980).

[65] R. J. Cook, Photon number statistics in resonance fluorescence, Phys. Rev. A **23**, 1243 (1981).

[66] H. J. Carmichael, S. Singh, R. Vyas, and P. R. Rice, Photoelectron waiting times and atomic state reduction in resonance fluorescence, Phys. Rev. A **39**, 1200 (1989).

[67] D. F. Walls and P. Zoller, Reduced quantum fluctuations in resonance fluorescence, Phys. Rev. Lett. **47**, 709 (1981).

[68] L. Mandel, Squeezed states and sub-poissonian photon statistics, Phys. Rev. Lett. **49**, 136 (1982).

[69] D. M. Keys, A quantum stochastic approach to Poisson master equation unravellings and Ghirardi-Rimini-Weber theory, Ph.D. thesis, The University of Arizona, 2022.

[70] N. Gisin and I. C. Percival, Quantum state diffusion: from foundations to applications, arXiv:quant-ph/9701024.

[71] I. Percival, *Quantum State Diffusion* (Cambridge University Press, Cambridge, UK, 1998).

[72] C. M. Natarajan, M. G. Tanner, and R. H. Hadfield, Superconducting nanowire single-photon detectors: physics and applications, Supercond. Sci. Technol. **25**, 063001 (2012).

[73] C.-K. Chou, C. Auchter, J. Lilieholm, K. Smith, and B. Blinov, Note: Single ion imaging and fluorescence collection with a parabolic mirror trap, Rev. Sci. Instrum. **88**, 086101 (2017).

[74] S. J. Jones, H. M. Wiseman, and A. C. Doherty, Entanglement, Einstein-Podolsky-Rosen correlations, Bell nonlocality, and steering, Phys. Rev. A **76**, 052116 (2007).

[75] H. M. Wiseman and J. M. Gambetta, Are dynamical quantum jumps detector dependent? Phys. Rev. Lett. **108**, 220402 (2012).

[76] S. Daryanoosh and H. M. Wiseman, Quantum jumps are more quantum than quantum diffusion, New J. Phys. **16**, 063028 (2014).

[77] A. Barchielli and M. Gregoratti, Quantum measurements in continuous time, non-Markovian evolutions and feedback, Philos. Trans. R. Soc. A **370**, 5364 (2012).

[78] S. Arranz Regidor, G. Crowder, H. Carmichael, and S. Hughes, Modeling quantum light-matter interactions in waveguide QED with retardation, nonlinear interactions, and a time-delayed feedback: Matrix product states versus a space-discretized waveguide model, Phys. Rev. Res. **3**, 023030 (2021).

[79] J. Preskill, Quantum computing in the NISQ era and beyond, Quantum **2**, 79 (2018).

[80] E. Altman, K. R. Brown, G. Carleo, L. D. Carr, E. Demler, C. Chin, B. DeMarco, S. E. Economou, M. A. Eriksson, K.-M. C. Fu, M. Greiner, K. R. A. Hazzard, R. G. Hulet, A. J. Kollár, B. L. Lev, M. D. Lukin, R. Ma, X. Mi, S. Misra, C. Monroe *et al.*, Quantum simulators: Architectures and opportunities, PRX Quantum **2**, 017003 (2021).

[81] J. Fraxanet, T. Salamon, and M. Lewenstein, The coming decades of quantum simulation, in *Sketches of Physics: The Celebration Collection*, Lecture Notes in Physics, Vol. 1000, edited by R. Citro, M. Lewenstein, A. Rubio, W. P. Schleich, J. D. Wells, and G. P. Zank (Springer International Publishing, 2023), pp. 85–125.

[82] B. Skinner, J. Ruhman, and A. Nahum, Measurement-induced phase transitions in the dynamics of entanglement, Phys. Rev. X **9**, 031009 (2019).

[83] Y. Li, X. Chen, and M. P. A. Fisher, Quantum Zeno effect and the many-body entanglement transition, Phys. Rev. B **98**, 205136 (2018).

[84] Y. Li, X. Chen, and M. P. A. Fisher, Measurement-driven entanglement transition in hybrid quantum circuits, Phys. Rev. B **100**, 134306 (2019).

[85] A. Chan, R. M. Nandkishore, M. Pretko, and G. Smith, Unitary-projective entanglement dynamics, Phys. Rev. B **99**, 224307 (2019).

[86] P. Sierant and X. Turkeshi, Universal behavior beyond multifractality of wave functions at measurement-induced phase transitions, Phys. Rev. Lett. **128**, 130605 (2022).

[87] X. Turkeshi, R. Fazio, and M. Dalmonte, Measurement-induced criticality in $(2+1)$-dimensional hybrid quantum circuits, Phys. Rev. B **102**, 014315 (2020).

[88] O. Lunt, M. Szyniszewski, and A. Pal, Measurement-induced criticality and entanglement clusters: A study of one-dimensional and two-dimensional Clifford circuits, Phys. Rev. B **104**, 155111 (2021).

[89] P. Sierant, M. Schirò, M. Lewenstein, and X. Turkeshi, Measurement-induced phase transitions in $(d+1)$-dimensional stabilizer circuits, Phys. Rev. B **106**, 214316 (2022).

[90] X. Cao, A. Tilloy, and A. D. Luca, Entanglement in a fermion chain under continuous monitoring, SciPost Phys. **7**, 024 (2019).

[91] G. Piccitto, A. Russomanno, and D. Rossini, Entanglement transitions in the quantum Ising chain: A comparison between different unravelings of the same Lindbladian, Phys. Rev. B **105**, 064305 (2022).

[92] M. Kolodrubetz, Optimality of Lindblad unfolding in measurement phase transitions, Phys. Rev. B **107**, L140301 (2023).

[93] X. Turkeshi, A. Biella, R. Fazio, M. Dalmonte, and M. Schiró, Measurement-induced entanglement transitions in the quantum Ising chain: From infinite to zero clicks, Phys. Rev. B **103**, 224210 (2021).

[94] P. Sierant and X. Turkeshi, Controlling entanglement at absorbing state phase transitions in random circuits, Phys. Rev. Lett. **130**, 120402 (2023).

[95] M. Buchhold, T. Müller, and S. Diehl, Revealing measurement-induced phase transitions by pre-selection, arXiv:2208.10506.

[96] T. Iadecola, S. Ganeshan, J. H. Pixley, and J. H. Wilson, Measurement and feedback driven entanglement transition in the probabilistic control of chaos, Phys. Rev. Lett. **131**, 060403 (2023).

[97] L. Piroli, Y. Li, R. Vasseur, and A. Nahum, Triviality of quantum trajectories close to a directed percolation transition, Phys. Rev. B **107**, 224303 (2023).

[98] N. O'Dea, A. Morningstar, S. Gopalakrishnan, and V. Khemani, Entanglement and absorbing-state transitions in interactive quantum dynamics, Phys. Rev. B **109**, L020304 (2024).

[99] V. Ravindranath, Y. Han, Z.-C. Yang, and X. Chen, Entanglement steering in adaptive circuits with feedback, Phys. Rev. B **108**, L041103 (2023).

[100] V. Ravindranath, Z.-C. Yang, and X. Chen, Free fermions under adaptive quantum dynamics, arXiv:2306.16595.

[101] P. Sierant and X. Turkeshi, Entanglement and absorbing state transitions in $(d+1)$-dimensional stabilizer circuits, Acta Phys. Pol. A, **144**, 415 (2023).